REMOTE SENSING LETTERS, 2016
VOL. 7, NO. 2, 170–179
http://dx.doi.org/10.1080/2150704X.2015.1117156

Taylor & Francis
Taylor & Francis Group

Automated extraction of ground surface along urban roads from mobile laser scanning point clouds

Bin Wu[a,b], Bailang Yu[a,b], Chang Huang[c], Qiusheng Wu[d] and Jianping Wu[a,b]

[a]Key Laboratory of Geographic Information Science, Ministry of Education, East China Normal University, Shanghai, China; [b]School of Geographic Sciences, East China Normal University, Shanghai, China; [c]College of Urban and Environmental Science, Northwest University, Xi'an, China; [d]Department of Geography, Binghamton University, State University of New York, Binghamton, NY, USA

ABSTRACT

Extracting ground surface from high-density point clouds collected by Mobile Laser Scanning (MLS) systems is of vital importance in urban planning and digital city mapping. This article proposes a novel approach for automated extraction of ground surface along urban roads from MLS point clouds. The approach, which was designed to handle both ordered and unordered MLS point clouds, consists of three key steps: constructing vertical profile from MLS point clouds along the vehicle trajectory; extracting candidate ground points using an adaptive alpha shapes algorithm; refining the candidate ground points with an elevation variance filter. To evaluate the performance of the proposed method, experiments were conducted using two types of urban street-scene point clouds. The results reveal that the ground points can be detected with an error rate of as low as 1.9%, proving that our proposed method offers a promising solution for automated extraction of ground surface from MLS point clouds.

ARTICLE HISTORY
Received 24 June 2015
Accepted 28 October 2015

1. Introduction

In recent decades, laser scanning technology has become one of the most efficient surveying techniques for acquiring detailed and accurate 3D data. The laser scanners can be deployed on platforms that are airborne, terrestrial or mobile. As an airborne laser scanning technology, light detection and ranging (LiDAR) has produced large volumes of highly accurate and densely sampled topographical measurements (1~5 m spatial resolution) (Wu et al. 2015). Mobile laser scanning (MLS) systems, an alternative platform for laser scanning, provide an even more accurate way for mapping topography, buildings, vegetation and other road objects in urban areas (Wu et al. 2013; Yu et al. 2010). With the increasing availability of MLS data, there is a call for automated algorithms and software tools for efficiently segmenting and extracting objects of interest from MLS point clouds (Yang and Fang 2014). However, due to the huge data volumes, variable point densities, complicated scene structures and occlusion of features by moving objects, automated segmentation and recognition of objects from MLS point clouds have become a big challenge (Yang and Fang 2014).

CONTACT Bailang Yu blyu@geo.ecnu.edu.cn Key Laboratory of Geographic Information Science, Ministry of Education, East China Normal University, Shanghai 200241, China

The extremely high density point clouds collected by MLS systems in urban areas might contain various types of objects, such as buildings, roads, cars, poles, pedestrians and trees. In general, the MLS point clouds can be classified into ground and non-ground points. Filtering out non-ground points and extracting ground points are essential for many road inventory studies (Pu et al. 2011; Yu et al. 2015). It helps to minimize the data volume and make the subsequent analysis efficient and straightforward (Yu et al. 2015). Extracting ground points from MLS point clouds mainly includes the procedure of differentiating 3D points that belong to ground surface from non-ground ones. Besides, other research has shown that the organization pattern (ordered or unordered) of the point clouds can be effected by mounting position of the laser scanner(s) (Lim et al. 2013). So far, many efforts have been made to address this problem. The existing ground-filtering approaches can be divided into several categories: morphological filter (Hernandez and Marcotegui 2009), linear prediction (Lam et al. 2010), triangulated irregular network (Jaakkola et al. 2008) and cluster (Biosca and Lerma 2008). However, these approaches mostly developed for unordered MLS point clouds have difficulty in handling complicated ground surfaces and induce high computational complexity (Zhou et al. 2014). More recently, the scan-line-based approach which detects local ground points with slope and elevation along a series of scanning lines was introduced by Hu, Li, and Zhang (2013) and Zhou et al. (2014). Although the scan-line-based approach has been proven to be efficient, there are still some limitations in dealing with unordered MLS point clouds which are lack of the characteristics of the scanning line's order.

In this article, we proposed a new approach for automated detection and segmentation of ground points from MLS point clouds acquired along urban roads. The contributions of the article are as follows: (1) an automated ground points extraction algorithm was designed to be applicable for both sloping ground and complex urban scenes irrespective of the organization pattern (ordered or unordered) of the input data set; (2) an adaptive version of alpha shapes algorithm was employed to detect candidate ground points.

2. Proposed algorithm

The proposed method consists of following three key steps.

2.1. *Vertical profile construction*

To reduce computation time and to make the point clouds manageable, a number of methods have been proposed to partition the MLS point clouds into consecutive road cross sections and their corresponding profiles at a certain interval (Yu et al. 2015; Yang, Fang, and Li 2013). These profiles were used as the basis for the further profile images generation which cannot represent the sharp surface fluctuations of ground surface. Therefore, the existing profile-generation methods are not suitable for ground points detection. Compared with those methods, the vertical profile construction we proposed is a continuous profiling process that partitions the raw point clouds into a series of sequential isometric strips and then generates 2D point sets after a centre plane projection. This process can handle both unordered and ordered MLS point clouds without missing details. It is an essential step for preparing data for subsequent analysis.

In order to illustrate the procedure of vertical profile construction, a local coordinate system needs to be defined first. It is defined using the following rules:

(1) The origin (O) of the local coordinate system is set at the first point of a trajectory segment.
(2) The *xy* horizontal plane: *x*-axis is along the direction of motion of the vehicle, while *y*-axis is perpendicular to the *x*-axis along the counterclockwise direction in the horizontal plane.
(3) *z*-axis points upward to form a right-handed coordinate system.

The direction of *x*-axis and *y*-axis could be changing from time to time, because the roads are not always straight. A common strategy to deal with these issues is to partition the point clouds into smaller straight segments along the road according to the trajectory points (Wu et al. 2013; Pu et al. 2011). For each small straight road segment (Figure 1(a)), the direction of *x*-axis can be determined by the corresponding trajectory points. Subsequently, the individual local coordinate system is constructed with the aforementioned rules. Sequential construction of the local coordinate systems from segment to segment along the road would improve the operating efficiency.

After the establishment of the local coordinate system, a series of strips $\{S_1, S_2, \ldots, S_n\}$ are created. Figure 1(a) illustrates the process of strips creation in a schematic scene with a plan view. Strips with an identical width of *d* are established along the direction perpendicular to the direction of motion of the vehicle trajectory on the *xy* plane. Figure 1(b) shows a real 3D view of the associated strips and the point clouds. After establishing the strips, all the points are carved up into different strips.

For each strip, the centre axis and the centre *yOz* plane are identified. The points located in each strip are projected to the centre *yOz* plane. Each point has the same *x* coordinate x_{S_i}; the plane point set can be described as $P_{S_i} = \{p_1, p_2, \ldots, p_m\}, i \in (1, 2, \ldots, n)$, in which a point $p_i (i = 1, 2, \ldots, m)$ is represented by (x_i, y_i, z_i) in the 3D coordinate system. Therefore, the point set lying in the *yOz* plane reflects the profile along the centre axis.

2.2. *Locally candidate ground points detection*

The concept of alpha shapes (*α*-shapes) was first introduced in the late 1980s as an attempt to define the shape of a point set on a plane (Edelsbrunner, Kirkpatrick, and Seidel 1983). It is a series of piecewise linear simple curves used to describe the polygonal contour of a finite set of points on the Euclidean plane. The alpha shapes have been widely used to find the outline of an unorganized set of data points (Da 2015; Edelsbrunner 2010).

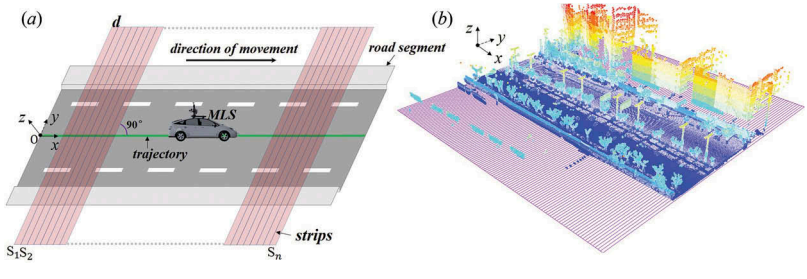

Figure 1. Sketch of the principle of strips construction for a road segment. (a) Strips construction; (b) 3D view of strips and point clouds.

According to Edelsbrunner (2010), the alpha shapes (ψ_T) of a finite spatial point set T can be defined as the intuitive notion of the boundary shape that contains all points of T. It is determined by the point set T and a positive number α, which controls the resulting shape of the boundary of T (Equation 1).

$$\psi_T = F(T,\alpha) \tag{1}$$

In general, larger α defines a more compact boundary of the point set. The alpha shapes approximate a common convex hull when α is near zero (Edelsbrunner 2010). The smaller the distance between adjacent points (high point density), the more compact will be the point set. Consequently, the value of α in areas with large distance between adjacent points (low point density) is smaller than those in regions with small distance (high point density). The alpha shapes algorithm works properly in finding the boundary points, but there are some limitations. For example, it is difficult to find a satisfying alpha value which would not exclude too many boundary points that reflect the detailed boundary structure. Therefore, we developed an adaptive alpha shapes algorithm based on the traditional algorithm.

In contrast to the traditional alpha shapes, the adaptive alpha shapes (E_{ψ_T}) which work on the point set P_{S_i} are determined by a function, F, which is based on four parameters (Equation 2): (1) a point set T; (2) a positive number α; (3) a constrained rotation angle θ and (4) a constrained process range L.

$$E_{\psi_T} = F(T,\alpha,\theta,L) \tag{2}$$

Here, E_{ψ_T} represents the boundary points and T is the point set P_{S_i}. The variable α is designed to control the level of detail reflected by the adaptive alpha shapes. It changes continuously when the adaptive alpha shapes algorithm is executing. If a neighbourhood of a point in T is the next/previous one of the point in the sequence after sorting based on the y coordinate, the α can be defined as the reciprocal of the planimetric Euclidean distance between the current point and the next neighbour (Edelsbrunner, Kirkpatrick, and Seidel 1983) (Equation 3):

$$\alpha = 1/\mathrm{dist}(p_i,p_{i+1}) \tag{3}$$

where dist() is a distance function that calculates the planimetric Euclidean distance between two points. If the minimum and maximum planimetric Euclidean distances between any two nearby points in point set P_{S_i} are R_{min} and R_{max} respectively, then α ranges from $1/R_{max}$ to $1/R_{min}$. The constrained rotation angle θ controls the slope of the segment of the adaptive alpha shapes which represent the local slope of the ground surface. As shown in Figure 2(b), $\theta = 0°$ is defined as the negative direction of z-axis and positive θ increases along a counterclockwise direction. The constrained process range L determines the range between the beginning and end points which are decided by the minimum and maximum y coordinate (L_{min} and L_{max}), respectively. Figure 2(a) shows a schematic example of the adaptive alpha shapes algorithm run as a ball-pivoting way. A ball pivots from L_{min} to L_{max}. First, a ball of an initial diameter $1/\alpha_{max}$ is placed at the beginning point (L_{min}). The ball cannot pass through the point set without touching its nearby points. In its pivoting motion, if there is no point hit by the ball in a given rotation angle range (0° to θ), α will be adaptive to a new value α_{new} by subtracting a certain interval α_{th} $((\alpha_{max} - \alpha_{min})/100)$. Then the size of the ball will be changed with the new value α_{new}. The new ball will pivot again to find whether a nearby point is hit or not. If yes, the hit point

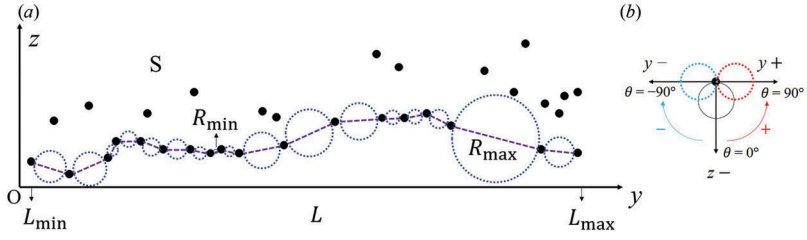

Figure 2. The adaptive alpha shapes. (a) A ball pivots from L_{min} to L_{max}. The pivoting ball is first placed in L_{min}. In its pivoting motion, if the ball hits one point in a given rotation angle range, the hit point will be marked and regarded as a start point to continue the searching process. Otherwise, the diameter of the ball will be changed with a new α value until the ball touches one point; (b) Definition of rotation angle θ.

will be marked as a candidate boundary point and used as a new starting point to repeat the aforementioned process. Otherwise, α will be recalculated until the ball touches one nearby point. The above process is repeated, round by round, until the ball reaches the end point (L_{max}) and finally all the candidate boundary points have been identified.

Here, the locally candidate ground points, which are used as the seed ground points in each strips, are identified in each individual point set P_{S_i} using the adaptive alpha shapes algorithm. The procedure mainly consists of following two components.

2.2.1. *Detection of the starting point of the ground.*

To get reliable starting point along the point set, the starting point should be determined by the location of the vehicle trajectory. As any position of the vehicle trajectory can be calculated, the intersection point of the vehicle trajectory and the profile plane can be estimated according to the coordinate x_{S_i}. For those points (x_{S_i},y_i,z_i) in the profile plane that are near the intersection, the one that satisfies the criterion defined in Equation 4 is selected as the starting ground point $p_{S_i}(x_{S_i},y_{S_i},z_{S_i})$ for the profile plane:

$$\{\min|z_{S_i}-z_i|\} \tag{4}$$

This rule makes the point lying below the intersection point with a minimum height difference is considered as the seed ground point.

2.2.2. *Execution of the adaptive alpha shapes algorithm.*

Considering the curbs, low vegetation and other road objects may exist on the road surface, the traditional slope-based method may lead to the omission errors for a fixed threshold. Therefore, we developed the adaptive alpha shapes algorithm to identify the remaining candidate ground points in the current sequence of points based on the position of the seed ground point. Since the seed ground point can be located anywhere within the point sequence, it is necessary to search both directions (Figure 3(a)). For each direction, the adaptive alpha shapes start from the seed point p_{S_i}, with α controlling the search radius and L_{min} together with L_{max} keeping the adaptive alpha shapes algorithm running within the constrained range. Whenever a qualified point is found, it will be added into the seed ground point set $G=\{p_{S_i},\ldots\}$ and used as the seed point for the next round of searching. If no qualified points are identified, the alpha adaptive shapes will adapt its size to repeat the searching, until it reaches the end (L_{min} or L_{max}).

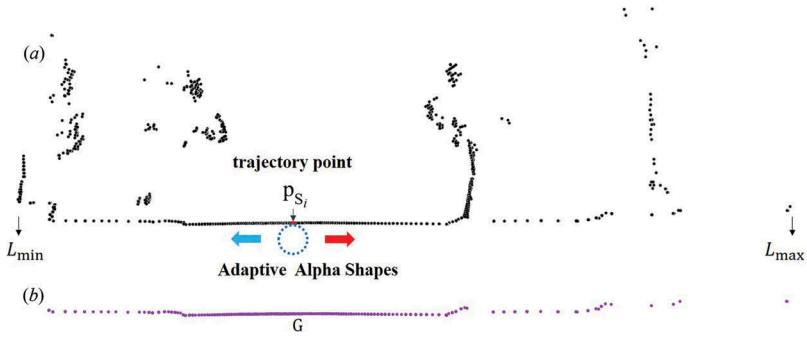

Figure 3. The ground points extraction. (a) The adaptive alpha shapes search both directions; (b) The extraction result.

It should be noted that when the urban objects are lower than the initial slope threshold δ_{th}, some candidate ground points extracted by the aforementioned procedure might actually belong to these non-ground objects. This issue often happens when the distance between two adjacent points is large. A validation process for those distant points is thus necessary. The point set G is first sorted according to the *y* coordinate. For any three neighbouring points which have significant difference of the *y* coordinate in the point set G, the following criterion should be satisfied:

$$\theta_{i,i+1} < \delta_{th} \text{ and } \theta_{i,i+2} < \delta_{th} \tag{5}$$

where $\theta_{i,i+1}$ represents the slope between two neighbouring points. Otherwise, the $(i + 2)$th point would be excluded from G because of the large slope $\theta_{i,i+2}$. The extraction result is showed in Figure 3(b).

2.3. *Elevation variance filtering*

The elevation variance filter was designed to optimize the coherence of ground points in the strip within a defined neighbourhood of each candidate ground point by filtering out non-ground points. The elevation variance D_{p_g} is defined by

$$D_{p_g} = E\left[(z - E[z])^2\right] (g = 1, 2, \ldots, k) \tag{6}$$

where p_g is the point in G; *z* represents the elevation of each point; *k* is the number of points in G and *E* represents the expectation. In general, a large elevation variance indicates an irregular topography, while a small elevation variance represents a relative flat site (e.g., ground surface).

For each $p_g\left(x_g, y_g, z_g\right)$, its neighbourhood is defined by a search radius threshold which equals the width, d, of the strip (S_i). All the points located in the neighbourhood are first sorted in ascending order of the elevation difference to z_g. Each sorted point is added into the Equation 6 in sequence for calculating the elevation variance. If the current elevation variance satisfies the criterion given by

$$D_{p_g} < D_{th} \tag{7}$$

where the threshold D_{th} is tolerance of elevation variance, the added point will be marked as ground point. The next point in the sorted point set is added to continue the next round of the variance calculation with the labelled ground points. If the criterion specified in Equation 7 is not satisfied, the process will stop and the remaining points will be marked as non-ground points. The above-mentioned process is repeated for each point in G. All strips from S_1 to S_n are processed sequentially with the elevation variance filter. Finally, the point clouds can be segmented into ground and non-ground parts.

The aforementioned step-wise extraction algorithm has been implemented using Microsoft Visual C#.NET programming language and ArcObjects SDK for .NET. In the algorithm, three parameters $\{d, \delta_{th}, D_{th}\}$ can be specified by the user, which will be discussed in Section 3.3.

3. Experimental results and discussion

3.1. *Input data and threshold selection*

Two case studies (Figure 4(a) and Figure 4(c)) are demonstrated to evaluate the validity of the proposed method. The MLS point clouds of Study Area I (Figure 4(a)) is an unordered data set acquired using a vehicle-mounted MLS system from East China Normal University (Wu et al. 2013). The MLS system was equipped with two laser scanners which have a valid scanning range of 80 m and a 180° field of view and one scanner heads upward while the other downward (Wu et al. 2013). The raw point clouds consist of 12,371,798 points covering a 4.5 km length urban street road and the average point density is 104 points/m^2. The Study Area II (Figure 4(c)) is a campus road and has a length of 913 m. The point clouds consist of 1,017,108 points and the average point density is 72 points/m^2. It is an ordered data set obtained from Carnegie Mellon University (CMU) which was collected using the Navlab11 vehicle equipped with side looking SICK LMS laser scanners (Munoz et al. 2009). Buildings and other urban objects, such as street trees, lights, curbs and cars, were distributed along the road. Both landscapes had flat ground as well as sloping ground. Considering the complexity of landscapes in these two study areas and the computational efficiency of the proposed algorithm, the following parameters were used: d = 0.2 m, δ_{th} = 20°, and D_{th}= 0.05.

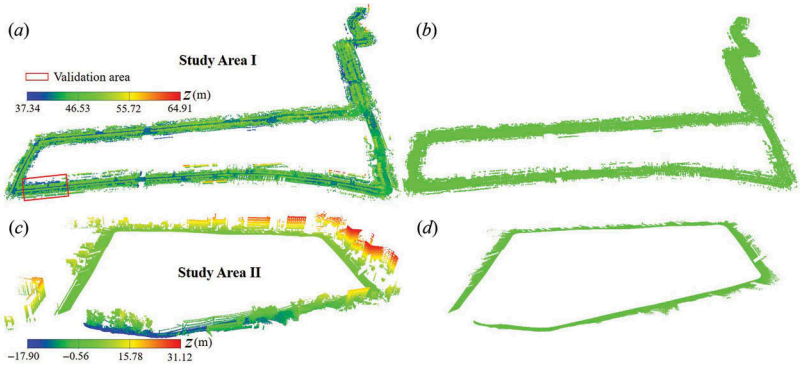

Figure 4. Case studies. (a) The original laser scanning point clouds of Study Area I; (b) Identified ground points of Study Area I; (c) The original laser scanning point clouds of Study Area II; (d) Identified ground points of Study Area II.

3.2. *Performance evaluation and comparison*

The results shown in Figure 4(b) and (d) demonstrated that the proposed method successfully extracted the ground points in both case studies. The details of the ground were well preserved.

According to Hu, Li, and Zhang (2013) and Zhou et al. (2014), the accuracy of ground points extraction algorithm can be evaluated by two types of errors: (1) rejection of the ground points (Type I error), and (2) acceptance of the non-ground points as ground points (Type II error). The point clouds in the Study Area II is a standard data set that has the segmentation label (hand-labelled) which can be directly used for verification. For the Study Area I, the manual segmentation result was used as the reference to calculate the error rate. The proposed method presents a total error rate of 3.561% (Type I error = 2.453% and Type II error = 1.108%) for Study Area I and 1.991% (Type I error = 1.124 % and Type II error = 0.867%) for Study Area II. This is comparable to the results reported in previous studies using ordered MLS point clouds (e.g., 0.674% reported by Zhou et al. (2014) and 8.240% reported by Hu, Li, and Zhang (2013)) and the results reported by using ALS point clouds (e.g., approximately 30% to 2% with nine ground filters tested on relative flat urban sites reported by Meng, Currit, and Zhao (2010)).

3.3. *Discussions*

The proposed method can be applied for both the ordered or unordered MLS point clouds. In the first step, the vertical profile construction procedure converting MLS point clouds into a series of vertical profiles is presented for reducing the dimension of complex data sets and making the computation manageable. An adaptive alpha shapes algorithm is employed to detect candidate ground points from the profiles. It achieves self-adaptability through a positive number α. There is no need to determine a fixed alpha value for the alpha shapes. Finally, an elevation variance filter is designed to identify ground points in the neighbourhood of each candidate ground point which ensures that the local slope of the ground surface is locally consistent and smooth.

Three parameters $\{\mathrm{d}, \delta_{\mathrm{th}}, D_{\mathrm{th}}\}$ need to be determined in the proposed method. The threshold d varies based on the input MLS point clouds. It might be difficult to automatically adjust the threshold d for different MLS point clouds without prior knowledge. In this study, a range of d (from 0.1 m to 1 m) for ground points extraction in the sample area (red box in Figure 4(a)) was conducted to evaluate its impact on the accuracy of the ground point extraction, and the results are shown in Table 1. It is clear that the Type I error rate increases when d changes from 0.1 m to 1 m and the Type II error rate is relatively stable when d changes from 0.2 m to 0.4 m. The results suggest that there is no significant change for the total error rate when d increases from 0.2 m to 0.4 m. For ordered MLS point clouds, d can be set to the distance between two neighbouring scanning lines, while for unordered data set, d can be determined by the point density. It is assigned to a larger value for low-density point clouds and a smaller value for high-density data. The parameter δ_{th} is decided by the degree of local roughness of the topography on the ground surface. Previous studies (e.g., Zhou et al. 2014; Hu, Li, and Zhang 2013) suggested that the parameter δ_{th} be set to 10°–20° for urban areas. The parameter D_{th} determines the quality of the extracted ground points. A large value for D_{th} will increase Type II error, while a small D_{th} will increase Type I

Table 1. The impact of the size of the strip width d on the accuracy of the ground point extraction.

d (m)	Type I error (%)	Type II error (%)	Total errors (%)
0.1	0.606	1.902	2.508
0.2	0.624	0.218	0.842
0.3	0.918	0.347	1.265
0.4	0.926	0.476	1.402
0.5	1.011	0.928	1.939
0.6	1.104	1.003	2.107
0.7	1.858	1.370	3.228
0.8	2.654	1.608	4.262
0.9	3.272	1.809	5.081
1.0	3.927	2.104	6.031

error, leading to an incomplete ground points extraction. Therefore, it is recommended to set a smaller D_{th} for relatively flat urban street and a larger D_{th} for rough urban street.

The two case study areas presented are typical street scenes in urban landscapes. By using the adaptive alpha shapes and elevation variance filter, there were only a few non-ground points that were falsely identified as ground points, and the Type II error rate is very low. The reason why the Type I error rate is higher than the Type II error rate is probably due to the existence of large gaps and isolated points in the point clouds. For urban surface with more complex structures, the pre-processing steps aforementioned would improve the extraction results. Besides, the continuity of the ground points could be influenced by higher urban objects as a result of the gap between two neighbouring ground points being larger than the normal distance. In this case, the isolated ground points would fail to be identified.

4. Conclusion

In this article, we proposed a novel approach for ground surface extraction in complex urban scenes from Mobile Laser Scanning (MLS) point clouds. It can be used for both ordered and unordered point clouds. This approach consists of three key steps: (1) the vertical profiles construction; (2) the locally candidate ground points detection and (3) the elevation variance filtering. More importantly, an adaptive version of alpha shapes algorithm for extracting candidate ground points is put forward. Two case study areas have been applied to evaluate the performance of the approach. The results demonstrated that the ground surface points can be extracted at a very high accuracy. We hope that this study could enlighten more applications of MLS point clouds in urban object extraction.

Acknowledgement

We thank Prof. Timothy Warner, Dr. Craig Cassells, and three anonymous reviewers for their constructive comments and suggestions.

Disclosure statement

No potential conflict of interest was reported by the authors.

Funding

This work was supported in part by the National Natural Science Foundation of China [grant number 41471449], in part by the Natural Science Foundation of Shanghai [grant number 14ZR1412200] and in part by the Fundamental Research Funds for the Central Universities of China.

References

Biosca, J. M., and J. L. Lerma. 2008. "Unsupervised Robust Planar Segmentation of Terrestrial Laser Scanner Point Clouds Based on Fuzzy Clustering Methods." *ISPRS Journal of Photogrammetry and Remote Sensing* 63 (1): 84–98. doi:10.1016/j.isprsjprs.2007.07.010.

Da, T. K. F. 2015. "2D Alpha Shapes." In *CGAL User and Reference Manual*, edited by CGAL Editorial Board. http://doc.cgal.org/latest/Alpha_shapes_2/index.html

Edelsbrunner, H. 2010. "Alpha Shapes—A Survey." In *Tessellations in the Sciences; Virtues, Techniques and Applications of Geometric Tilings*, edited by R. van de Weijgaert, G. Vegter, J. Ritzerveld, and V. Icke. Heidelberg: Springer Verlag.

Edelsbrunner, H., D. Kirkpatrick, and R. Seidel. 1983. "On the Shape of a Set of Points in the Plane." *IEEE Transactions on Information Theory* 29 (4): 551–559. doi:10.1109/TIT.1983.1056714.

Hernandez, J., and B. Marcotegui. 2009. "Filtering of Artifacts and Pavement Segmentation from Mobile LiDAR Data." ISPRS Workshop Laserscanning 2009, Paris, September 1–2.

Hu, X., X. Li, and Y. Zhang. 2013. "Fast Filtering of Lidar Point Cloud in Urban Areas Based on Scan Line Segmentation and GPU Acceleration." *IEEE Geoscience and Remote Sensing Letters* 10 (2): 308–312. doi:10.1109/LGRS.2012.2205130.

Jaakkola, A., J. Hyyppä, H. Hyyppä, and A. Kukko. 2008. "Retrieval Algorithms for Road Surface Modelling Using Laser-Based Mobile Mapping." *Sensors* 8 (9): 5238–5249. doi:10.3390/s8095238.

Lam, J., K. Kusevic, P. Mrstik, R. Harrap, and M. Greenspan. 2010. "Urban Scene Extraction from Mobile Ground Based LiDAR Data." 3DPVT 2010: 5th International Symposium on 3D Data, Processing, Visualization & Transmission, Paris, May 17–20, 1–8.

Lim, S., C. A. Thatcher, J. C. Brock, D. R. Kimbrow, J. J. Danielson, and B. J. Reynolds. 2013. "Accuracy Assessment of a Mobile Terrestrial Lidar Survey at Padre Island National Seashore." *International Journal of Remote Sensing* 34 (18): 6355–6366. doi:10.1080/01431161.2013.800658.

Meng, X., N. Currit, and K. Zhao. 2010. "Ground Filtering Algorithms for Airborne LiDAR Data: A Review of Critical Issues." *Remote Sensing* 2 (3): 833–860. doi:10.3390/rs2030833.

Munoz, D., J. A. Bagnell, N. Vandapel, and M. Hebert. 2009. "Contextual Classification with Functional Max-Margin Markov Networks." IEEE Conference on Computer Vision and Pattern Recognition (CVPR), Miami Beach, FL, June 20–25, 975–982.

Pu, S., M. Rutzinger, G. Vosselman, and S. O. Elberink. 2011. "Recognizing Basic Structures from Mobile Laser Scanning Data for Road Inventory Studies." *ISPRS Journal of Photogrammetry and Remote Sensing* 66 (6): S28–S39. doi:10.1016/j.isprsjprs.2011.08.006.

Wu, B., B. Yu, W. Yue, S. Shu, W. Tan, C. Hu, Y. Huang, J. Wu, and H. Liu. 2013. "A Voxel-Based Method for Automated Identification and Morphological Parameters Estimation of Individual Street Trees from Mobile Laser Scanning Data." *Remote Sensing* 5 (2): 584–611. doi:10.3390/rs5020584.

Wu, Q., H. Liu, S. Wang, B. Yu, R. Beck, and K. Hinkel. 2015. "A Localized Contour Tree Method for Deriving Geometric and Topological Properties of Complex Surface Depressions Based on High-Resolution Topographical Data." *International Journal of Geographical Information Science* 29 (12): 2041–2060.

Yang, B., and L. Fang. 2014. "Automated Extraction of 3-D Railway Tracks from Mobile Laser Scanning Point Clouds." *IEEE Journal of Selected Topics in Applied Earth Observations and Remote Sensing* 7 (12): 4750–4761. doi:10.1109/JSTARS.2014.2312378.

Yang, B., L. Fang, and J. Li. 2013. "Semi-Automated Extraction and Delineation of 3D Roads of Street Scene from Mobile Laser Scanning Point Clouds." *ISPRS Journal of Photogrammetry and Remote Sensing* 79: 80–93. doi:10.1016/j.isprsjprs.2013.01.016.

Yu, B., H. Liu, J. Wu, Y. Hu, and L. Zhang. 2010. "Automated Derivation of Urban Building Density Information Using Airborne Lidar Data and Object-Based Method." *Landscape and Urban Planning* 98 (3–4): 210–219. doi:10.1016/j.landurbplan.2010.08.004.

Yu, Y., L. Jonathan, H. Guan, C. Wang, and J. Yu. 2015. "Semiautomated Extraction of Street Light Poles From Mobile LiDAR Point-Clouds." *IEEE Transactions on Geoscience and Remote Sensing* 53: 1374–1386. doi:10.1109/TGRS.2014.2338915.

Zhou, Y., D. Wang, X. Xie, Y. Ren, G. Li, Y. Deng, and Z. Wang. 2014. "A Fast and Accurate Segmentation Method for Ordered LiDAR Point Cloud of Large-Scale Scenes." *IEEE Geoscience and Remote Sensing Letters* 11 (11): 1981–1985. doi:10.1109/LGRS.2014.2316009.